Binding of the Fap2 Protein of *Fusobacterium nucleatum* to Human Inhibitory Receptor TIGIT Protects Tumors from Immune Cell Attack

Chamutal Gur[1,2], **Yara Ibrahim**[3], **Batya Isaacson**[1], **Rachel Yamin**[1], **Jawad Abed**[3], **Moriya Gamliel**[1], **Jonatan Enk**[1], **Yotam Bar-On**[1], **Noah Stanietsky-Kaynan**[1], **Shunit Coppenhagen-Glazer**[3], **Noam Shussman**[4], **Gideon Almogy**[4], **Angelica Cuapio**[5], **Erhard Hofer**[5], **Dror Mevorach**[2], **Adi Tabib**[2], **Rona Ortenberg**[6], **Gal Markel**[6], **Karmela Mikli** [7], **Stipan Jonjic**[7], **Caitlin A. Brennan**[8], **Wendy S. Garrett**[8,9], **Gilad Bachrach**[3,10,*], and **Ofer Mandelboim**[1,10,*]

[1]The Lautenberg Center of General and Tumor Immunology, The Hebrew University Hadassah Medical School, IMRIC Jerusalem, 91120, Israel

[2]The Rheumatology Research Center, Hadassah-Hebrew University, Jerusalem, 91120, Israel

[3]The Institute of Dental Sciences, The Hebrew University-Hadassah School of Dental Medicine, Jerusalem, 91120, Israel

[4]Department of General Surgery, Hadassah-Hebrew University Medical Center, Jerusalem, 91120, Israel

[5]Department of Vascular Biology and Thrombosis Research Medical University of Vienna, 1090, Austria

[6]Ella Institute of Melanoma, Sheba Medical Center, Ramat-Gan, 526260, Israel

[7]Department of Histology and Embryology Center for Proteomics, Faculty of Medicine, University of Rijeka, 51000, Croatia

[8]Harvard School of Public Health, Boston, MA, 02115, USA

[9]Dana-Farber Cancer Institute, Boston, MA, 02115, USA

SUMMARY

Bacteria, such as *Fusobacterium nucleatum*, are present in the tumor microenvironment. However, the immunological consequences of intra-tumoral bacteria remain unclear. Here, we have shown that natural killer (NK) cell killing of various tumors is inhibited in the presence of various *F. nucleatum* strains. Our data support that this *F. nucleatum*-mediated inhibition is mediated by human, but not by mouse TIGIT, an inhibitory receptor present on all human NK cells and on various T cells. Using a library of *F. nucleatum* mutants, we found that the Fap2 protein of *F.*

[*]Correspondence: giladba@ekmd.huji.ac.il (G.B.), oferm@ekmd.huji.ac.il (O.M.).
[10]Co-senior author

nucleatum directly interacted with TIGIT, leading to the inhibition of NK cell cytotoxicity. We have further demonstrated that tumor-infiltrating lymphocytes expressed TIGIT and that T cell activities were also inhibited by *F. nucleatum* via Fap2. Our results identify a bacterium-dependent, tumor-immune evasion mechanism in which tumors exploit the Fap2 protein of *F. nucleatum* to inhibit immune cell activity via TIGIT.

Graphical Abstract
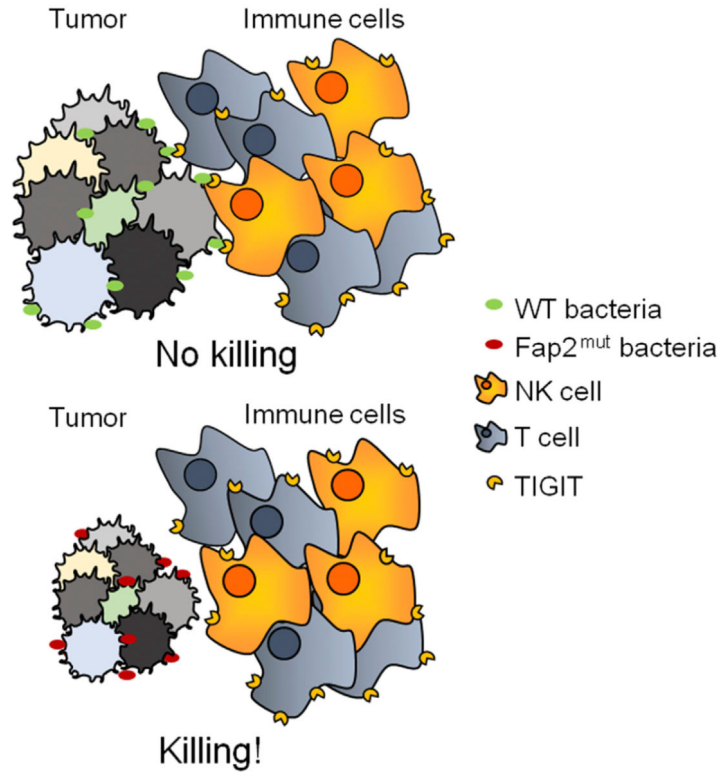
INTRODUCTION

Bacteria colonize nearly all human body surfaces, and the bacterial communities of the gastro-intestinal tract are the most abundant and complex (Tannock, 2008). This results in dynamic interplay between a host and its resident microbes, and the gut microbiota engage in a range of symbiotic interactions with the human mucosal immune system. There is an increasing appreciation that the gut microbiota might contribute to the pathogenesis of a range of human diseases. Coley's toxin, a mixture of killed bacteria including *Streptococcus pyogenes* and *Serratia marcescens*, is considered a forerunner of modern immunotherapy. Coley's toxin induces tumor regression in sarcomas and other solid tumors. However, the relationship between bacteria and tumors is multifactorial. In particular, compelling links are beginning to emerge between bacteria, inflammation, and many malignancies, especially colon adenocarcinoma (Jobin, 2013; Sears and Garrett, 2014). Fusobacteria are often enriched in patients with intestinal inflammation and cancer (Sobhani et al., 2011; Strauss et

al., 2011). It is still largely unknown why certain tumors are enriched with particular bacteria and whether such bacteria protect developing tumors from immune cell attack.

F. nucleatum is a common oral anaerobic Gram-negative rod and is primarily a periodontal bacterium. Interest in this bacterium has increased in the last few years because of its association with preterm birth (Han et al., 2004; Liu et al., 2007), colon adenocarcinoma (Castellarin et al., 2012; Kostic et al., 2013; Kostic et al., 2012; Rubinstein et al., 2013), and rheumatoid arthritis (Han and Wang, 2013; Témoin et al., 2012).

F. nucleatum directly engages with the immune system. Fusobacteria-associated Stillbirth and preterm births in mouse models are Toll-like receptor-4 (TLR4)-dependent (Liu et al., 2007). *F. nucleatum* also induces activation of intracellular RIG-I receptor, a sensor of RNA viruses (Lee and Tan, 2014). We have previously demonstrated that *F. nucleatum* directly interacts with the NK cell receptor NKp46 and observed that this interaction influences the outcome of *F. nucleatum*-mediated periodontitis (Chaushu et al., 2012).

NK cells are part of the innate immune system, although recent evidence suggests that they may also possess adaptive immune properties (Vivier et al., 2011). NK cells kill tumors, viruses, parasites and bacteria directly and indirectly (Koch et al., 2013). NK cell activity is controlled by a balance of signals, delivered by inhibitory and activating NK cell receptors (Koch et al., 2013). There are several activating NK cell receptors that recognize various ligands, which can be stress-induced, self-molecules, viral components or tumor proteins (Koch et al., 2013; Seidel et al., 2012). However, the exact mechanisms by which NK cells recognize and eliminate tumors via activating receptors are not well-understood, in part, because the tumor ligands of several activating NK cell receptors are unknown. In contrast, the identity of the ligands recognized by inhibitory NK cell receptors is very well defined. NK cells express a vast repertoire of inhibitory receptors (Gardiner, 2008; Gonen-Gross et al., 2010; Koch et al., 2013; Lankry et al., 2010; Seidel et al., 2012). Most of these inhibitory receptors belong to the KIR (Killer Inhibitory Receptors) family, recognizing both classical and non-classical major histocompatibility complex (MHC) class I proteins (Koch et al., 2013; Seidel et al., 2012). KIRs are stochastically expressed on the NK cell surface, and thus NK cells in a given individual express selected KIRs (Koch et al., 2013; Seidel et al., 2012). NK cells also express additional inhibitory receptors that do not recognize MHC class I proteins, such as CEACAM1, CD300a, and TIGIT (T cell immunoglobulin and ITIM domain) (Koch et al., 2013; Seidel et al., 2012).

The TIGIT receptor in humans is expressed on all NK cells, as well as on other immune cells (Stanietsky et al., 2009). It recognizes two very well-defined ligands: PVR and nectin2 (Stanietsky et al., 2009). The recognition of these ligands leads to the delivery of an inhibitory signal mediated by two motifs present in the cytoplasmatic tail of TIGIT: the immunoreceptor tail tyrosine (ITT)-like and the immunodominant tyrosine-based inhibitory (ITIM) motifs (Liu et al., 2013; Stanietsky et al., 2013; Stanietsky et al., 2009). In this study, we show that the Fap2 protein of *F. nucleatum* inhibits tumor cell killing by immune cells via TIGIT.

RESULTS

F. nucleatum Adheres to Various Tumor Cells and Inhibits NK Cell Cytotoxicity

F. nucleatum is found in human tumors, particularly colon adenocarcinoma tumors (Castellarin et al., 2012; Kostic et al., 2012). To test whether the origin of the tumor (epithelial versus hematopoietic) is important for *F. nucleatum* binding, we used FITC labeled *F. nucleatum* ATCC strain 23726 (herein named 726) and examined its binding to the human Epstein Bar Virus (EBV) transformed B cell line 721.221, to the human erythroleukemic line K562, and to the human colorectal carcinoma cell line RKO (Figure 1). We observed that *F. nucleatum* bound all the tumor cell lines tested (Figures 1A, 1D, and 1F). Using scanning electron microscopy (SEM), we observed that NK cells (designated E for effectors) clustered around *F. nucleatum* (designated B for bacteria) coated tumor cells (designated T for tumors) (Figure 1B).

We next tested whether *F. nucleatum* affects human NK cell cytotoxicity. Primary activated human NK cells were incubated for 5 hr with the various tumor cell lines that were pre-incubated with or without *F. nucleatum*, in medium containing penicillin and streptomycin (to ensure that *F. nucleatum* were not viable over the course of the assay). In the presence of *F. nucleatum*, there was a significant inhibition of NK cytotoxicity, irrespective of the human tumor cell line evaluated (Figures 1C, 1E, and 1G). To test whether this effect was specific to this particular *F. nucleatum* strain, we FITC labeled another *F. nucleatum* strain, ATCC 49256 *subsp. Vincentii* (herein named 492). We confirmed that it bound to 721.221 cells (Figure 1H) and observed that 492 also inhibited human NK cell killing (Figure 1I). In contrast, the ur-opathogenic *Escherichia coli* (UPEC) strain CFT073 did not inhibit NK cell cytotoxicity (Figure 1I). Incubation of the various cancer cell targets coated with the various *F. nucleatum* strains did not affect NK cell interferon-γ (IFN-γ) and tumor necrosis factor-α (TNF-α) secretion.

F. nucleatum Interacts with TIGIT

F. nucleatum-mediated inhibition of NK cell killing was observed when several cell lines were used and was reproducible using bulk primary activated human NK cells obtained from various donors. Consequently, we hypothesized that *F. nucleatum* might interact with an inhibitory NK cell receptor which is expressed on the entire NK cell population and whose expression is conserved across different individuals. As far as we know, TIGIT, (but not for example the KIR receptors), is the only NK inhibitory receptor which uniquely meets these requirements (Stanietsky et al., 2009). To test whether *F. nucleatum* interacts with TIGIT, we used a reporter system that we had previously generated (Stanietsky et al., 2009). Murine thymoma BW cells were transfected with a chimeric TIGIT protein in which the extracellular portion of human TIGIT (hTIGIT) is fused to the mouse zeta chain of the CD3 complex (Figure 2A, left). In this reporter system, if TIGIT is bound and triggered by a specific ligand, then mouse IL-2 is secreted. Thus, it reports both on the binding and on the functionality of these interactions. We previously used this system to demonstrate that both PVR and nectin2 are ligands for human and mouse TIGIT (Stanietsky et al., 2013; Stanietsky et al., 2009). As a control, we used BW cells expressing NKp30 fused to the mouse zeta chain of the CD3 complex (Figure 2A, right). The two reporter cells (BW

hTIGIT and BW NKp30), as well as the parental BW cells, were incubated with the 726 strain. Mouse interleukin-2 (IL-2) was detected only upon incubation of 726 with BW hTIGIT (Figure 2B), indicating that *F. nucleatum* binds to and activates hTIGIT. Because both TIGIT and DNAM1 bind to a shared ligand, PVR (Stanietsky et al., 2009), we also prepared another reporter cell line expressing the extracellular portion of DNAM1 fused to mouse zeta chain of the CD3 complex and observed that *F. nucleatum* did not interact with DNAM1 (Figure 2B). The TIGIT binding was not restricted to 726 bacteria, because the 492 strain also activated BWhTIGIT (Figure 2C). To test whether *F. nucleatum* could also bind mouse TIGIT, the mouse TIGIT (mTIGIT) protein fused to the mouse zeta chain was also expressed in BW cells (Figure 2D). However, no IL-2 secretion was detected when the mTIGIT was used (Figure 2E). Thus, we concluded that *F. nucleatum* directly interacts with human, but not mouse, TIGIT.

F. nucleatum Inhibits NK Cytotoxicity via TIGIT

To test whether *F. nucleatum* inhibits NK cell cytotoxicity via TIGIT, we initially used the YTS ECO tumor cell line. The TIGIT-negative YTS ECO cell line (Figure 3A) is an NK tumor cell line that does not express any known NK inhibitory receptors. YTS ECO kills only few cell lines, e.g., 721.221, which express CD48, but not K562 or RKO (which express little or no CD48). This is because the 2B4 activating receptor, which recognizes CD48, is the primary activating receptor that functions on the YTS ECO cell line (Elias et al., 2014). To test whether TIGIT inhibits YTS ECO cytotoxicity upon interaction with *F. nucleatum*-coated 721.221 cells, we expressed hTIGIT in YTS ECO cells (herein named YTS hTIGIT, Figure 3A). As a control, we expressed the known TIGIT ligand, PVR (Stanietsky et al., 2009), in 721.221 cells (Figure 3B). Next, we used the 721.221 and 721.221 PVR cells, incubated with and without the 726 strain, in killing assays. Although YTS ECO killing was not affected by the presence or absence of *F. nucleatum* (Figure 3C), the killing of YTS ECO cells expressing TIGIT was inhibited (Figure 3D). This inhibition was less pronounced as compared to the PVR inhibition (Figure 3D). To test whether *F. nucleatum* interacts with TIGIT at the same binding site that mediates PVR binding, we used a blocking antibody (#4) that was previously shown to block the hTIGIT interaction with PVR (Stanietsky et al., 2009). 721.221 cells were incubated with YTS hTIGIT cells in the presence or absence of *F. nucleatum* and in the presence or absence of anti-hTIGIT mAb #4. Although mAb #4 partially blocked the PVR-TIGIT interaction and consequently partially restored YTS hTIGIT cytotoxicity, it did not affect the *F. nucleatum*-mediated inhibition (Figure 3E). Taken together, these results suggest that *F. nucleatum* binds hTIGIT at a binding site distinct from that of human PVR.

TIGIT delivers its inhibitory signals via ITIM and ITT motifs located in its cytoplasmic tail (Liu et al., 2013; Stanietsky et al., 2013; Stanietsky et al., 2009). To corroborate our observations and to demonstrate that *F. nucleatum* also exerts its inhibitory effect on TIGIT through these motifs, we used two TIGIT truncation stop mutants (Stanietsky et al., 2009). One was a mutation at position 190 (named YTS hTIGIT stop 190, Figure 3F) lacking both ITT and ITIM motifs. The second was a mutation at position 231, in which a stop codon was inserted instead of the tyrosine residue of the ITIM motif (named YTS hTIGIT stop 231, Figure 3F). When either of the stop mutants were used, the *F. nucleatum*-inhibition of

TIGIT was abrogated (Figures 3G and 3H), suggesting that TIGIT's signaling inhibitory motifs are required for *F. nucleatum*-mediated inhibition.

To demonstrate that *F. nucleatum* inhibits primary human NK cytotoxicity via TIGIT, we incubated primary activated human NK cells with 721.221 (Figure 4A) or with RKO cells (Figure 4B) that were coated with or without *F. nucleatum* 726. NK cytotoxicity was inhibited in the presence of the bacterium (Figures 4A and 4B). To demonstrate that this inhibition was due to TIGIT, we blocked the *F. nucleatum* interaction using a fusion protein composed of the extracellular portion of hTIGIT fused to human IgG1 (TIGIT-Ig). The *F. nucleatum*-mediated inhibition was partially, but significantly, abolished when incubated in the presence of TIGIT-Ig, but not in the presence of a control Ig-fusion protein (C-Ig, Figures 4A and 4B).

To demonstrate that *F. nucleatum* strains from human colon tumors also inhibit NK cell cytotoxicity via TIGIT, we used *F. nucleatum* strains isolated from human colon adenocarcinoma. tumors. We next incubated 721.221 cells with two clinical strains and then incubated the cells coated with the bacteria with YTS hTIGIT cells (Figure 4C). Inhibition was observed with the *F. nucleatum* strain clinical tumor isolate (CTI)-2 but not with CTI-7 (Figure 4C). To further evaluate these results, we incubated the clinical strains CTI-7 and CTI-2 with the BW hTIGIT reporter system described above. In agreement with the killing results (Figure 4C), the CTI-2 but not the CTI-7 directly activated the BW hTIGIT cells (Figure 4D). Examination of the biological properties of these clinical strains revealed that the CTI-7 strain that was unable to inhibit YTS hTIGIT cytotoxicity (Figure 4C) and was unable to interact with TIGIT (Figure 4D) caused little or no hemagglutination (Figure 4E), whereas the CTI-2 strain, that inhibited YTS hTIGIT cytotoxicity (Figure 4C) and that interacted with TIGIT (Figure 4D), efficiently hemagglutinated human red blood cells (Figure 4E). Together, these results suggest that *F. nucleatum* inhibits NK ell cytotoxicity via TIGIT and that this inhibition is abrogated when *F. nucleatum* is unable to agglutinate red blood cells.

The Fusobacterial Fap2 Protein Interacts with TIGIT

To identify the *F. nucleatum* element that interacts with TIGIT, we generated a *F. nucleatum* transposon-based insertion-inactivation mutant library (Coppenhagen-Glazer et al., 2015). Library mutants were incubated with 721.221 cells and then with YTS hTIGIT cells, and inhibition of cytotoxicity was assayed. Mutants unable to cause inhibition of YTS hTIGIT cytotoxicity were tested for their ability to agglutinate red blood cells as we observed that TIGIT inhibition is abrogated in the absence of *F. nucleatum* hemagglutination (Figures 4C–4E; examples are shown in Figures 5A and 5B). Two mutants (K50 and D22) that were unable to inhibit the killing of YTS hTIGIT cells (Figure 5A) were also unable to cause hemagglutination (Figure 5B). We FITC labeled the K50 and D22 mutants and tested their binding to various cells lines. While we observed equal binding of the wild-type *F. nucleatum* and the two mutants, K50 and D22, to 721.221 cells at all ratios of bacteria to human cells tested (Figure 5C and Figure S1, in Figure 5C we show the MOI of 600 and the unstained 721.221 cells that also appear in Figure S1), the binding of the mutants to K562 and RKO cells was less efficient (especially in the low bacteria to human cell ratio) as

compared to wild-type *F. nucleatum* (Figure S1). We therefore continued our assays with 721.221 cells and observed that *F. nucleatum*-mediated inhibition of primary activated human NK cell killing was lost with the K50 and D22 mutants (Figure 5D). Furthermore, the K50 and D22 mutants were almost completely unable to activate the BW hTIGIT reporter system (Figure 5E).

In both K50 and D22 mutants, the transposon was inserted into the gene encoding for the Fap2 protein of *F. nucleatum* (Coppenhagen-Glazer et al., 2015). The insertions resulted in abolishment of the Fap2 protein expression as seen by Coomassie gel staining (Figure 6A). To demonstrate that TIGIT and Fap2 interact with each other, we used two assays. We used an ELISA-based assay in which the wild-type *F. nucleatum* and the two mutants K50 and D22 were bound to plates and then incubated with TIGIT-Ig. TIGIT interacted with the wild-type *F. nucleatum*, but not with the two mutants or with other bacteria, e.g., UPEC (Figure 6B). We also prepared a DNAM1-Ig (CD227-Ig) fusion protein and showed that it did not interact with the 726 bacterium (Figure 6B). Finally, we isolated vesicles derived from the outer membranes of wild-type *F. nucleatum* and the Fap2 mutant K50 and performed immunoblots with TIGIT-Ig on protein lysates from these vesicles fractions. TIGIT bound the wild-type *F. nucleatum* vesicles, whereas no binding was detected in the vesicles from the Fap2-deficient K50 strain (Figure 6C).

Lymphocytes within Tumors Express TIGIT and Are Inhibited in a Fap2-Dependent Manner

Because TIGIT is expressed on T lymphocytes, as well as on NK cells, we tested whether TIGIT is expressed in tumor infiltrating lymphocytes (TILs) found within colon adenocarcinoma and examined whether *F. nucleatum* inhibited the activity of these TILs in a Fap2-dependent manner. To stainTIGIT in situ, we developed another TIGIT-specific mAb (#1) and stained frozen sections of human colon adenocarcinomas. We observed that the TILs were broadly distributed throughout the colon adenocarcinoma sections and that TIGIT was expressed on the vast majority of TILs (Figure 7A). We next isolated the TILs from the colon adenocarcinomas and observed that NK cells constitute between 1%–5% of all TILs and that around half of the CD3$^+$ cells were CD8$^+$ and half were CD4$^+$. We also observed, in agreement with the immunofluorescence microscopy data (Figure 7A), that the vast majority of the TILs (NK, CD4$^+$, and CD8$^+$) express TIGIT (Figure 7B). However, because we were able to recover only a small number of TILs, we were unable to evaluate their functionality. Because the *F. nucleatum*-mediated inhibition of NK cell activities was observed with all NK cells tested, we reasoned that *F. nucleatum* would also inhibit T cell activities, irrespective of their origin. Therefore, to test whether *F. nucleatum* inhibits cytotoxic T lymphocyte (CTL) and T helper cell activities, we used TILs obtained from melanomas, a tumor type from which we have been able to isolate larger numbers of viable TILs and generate TIL cell lines. TIL #14 isolated from melanoma patient #14 is a CTL line that expresses TIGIT (Figure 7C). Other TILs isolated from melanoma patients, both CD4$^+$ and CD8$^+$, were also TIGIT positive. TIL #14 was incubated with the melanoma tumor #14 in the presence or in the absence of the various bacteria, and killing assays were performed. TIL #14 killing was inhibited in a Fap2-dependent manner, as moderate inhibition was observed with the 726 strain and this inhibition was abrogated in the absence of Fap2 (K50 mutant, Figure 7D). The Fap2-mediated TIGIT inhibition was dependent on the

hemagglutination activity of the bacteria. Strong inhibition (Figure 7D) was observed with bacteria that caused efficient hemagglutination (Figure 4E and 5B), moderate inhibition (Figure 7D) was observed with the 726 strain that caused moderate hemagglutination (Figure 5B), and no inhibition was observed with bacteria that caused little or no hemagglutination (Figure 4E and 5B).

We next tested whether *F. nucleatum* could inhibit the activity of T cells present in the peripheral blood. Because TIGIT is expressed on CD4^{+} memory T cells (Stanietsky et al., 2009), we incubated lymphocytes obtained from donors that were sero-positive or sero-negative for human cytomegalovirus (HCMV), with pp65 overlapping peptides in the presence or in the absence of the various *F. nucleatum* strains. Inhibition of IFN-γ secretion was observed with the Fap2-dependent bacteria (726, and CTI-2, Figure 7E). Again, the efficacy of inhibition correlated with the hemagglutination efficiency: moderate inhibition was observed with bacteria able to cause moderate hemagglutination (726, Figure 7E). Bacteria unable to hemagglutinate (K50 or CTI-7, Figures 4E and 5B) showed little or no inhibition of T cell activity (Figure 7E). No response was detected in donors sero-negative for HCMV (Figure 7E).

We further tested whether the presence or absence of Fap2 affected NK cell activity indirectly via the secretion of cytokines from dendritic cells (DCs). We incubated DCs with the 726 strain, the 492 strain, or with the Fap2 inactivated strain K50. There was equivalent secretion of IL-12 from the DCs, regardless of the *F. nucleatum* used (Figure 7F). We also incubated the cell culture supernatants of the DCs incubated with the *F. nucleatum* strains with primary human NK cells and observed a similar secretion of IFN-γ and TNF-α (Figures 7G and 7H, respectively). Thus, our data support that absence of Fap2 does not affect DC production of IL-12 or DC-mediated activation of NK cell-cytokine secretion and that the Fap2 of *F. nucleatum* serves as a modulator of tumor cell evasion by binding to TIGIT.

DISCUSSION

Immune evasion is a hallmark of cancer (Hanahan and Weinberg, 2011); however, whether bacteria within tumors provide tumors immune evasion properties is unknown. There is a dichotomy in the relationship between bacteria and cancer. In the early 1890s, the surgeon William Coley used bacteria and bacterial extracts to enhance anti-tumor immunity and successfully treated sarcoma patients (Coley, 1910). Today, instillation of *Mycobacterium bovis* Bacillus Calmette-Guérin (BCG) into the bladder is a standard treatment for non-muscle invasive bladder cancer (Grange et al., 2008). However, our data support that there might be bacteria found within tumors that facilitate a tumor's ability to evade immune cell attack. Bacteria found within tumors, for example *F. nucleatum*, were shown to promote tumor proliferation and enhance tumor progression (Jobin, 2013; Sears and Garrett, 2014). Herein, we have described and characterized a mechanism by which the human colon adenocarcinoma-associated bacterium *F. nucleatum* facilitates a tumor's evasion of the immune system. We have shown that *F. nucleatum* bound tumor cells and that *F. nucleatum*-containing tumors inhibited NK cell cytotoxicity and tumor infiltrating lymphocyte cell activities via the interaction of the *F. nucleatum* protein Fap2 with human TIGIT.

F. nucleatum seems well-adapted to its host-species as our human-derived *F. nucleatum* strains associated with human but not mouse TIGIT. These results are in line with our previous observations that hTIGIT manifests a broader recognition pattern than mTIGIT. Human TIGIT recognizes both the mouse and human PVR, whereas mTIGIT recognizes only mouse PVR (Stanietsky et al., 2013; Stanietsky et al., 2009). The lack of mTIGIT binding to *F. nucleatum* also explains prior observations in mouse models wherein *F. nucleatum*'s interaction with NCR1 led to increased periodontitis (Chaushu et al., 2012).

Current microbiome surveys of human tumors support that *F. nucleatum* is enriched in colon adenocarcinoma (Castellarin et al., 2012; Kostic et al., 2012). We found that the vast majority of TILs found within colon adenocarcinoma expressed TIGIT. The TILs were broadly distributed throughout the tissue sections and were not restricted to the specific sites in which the bacteria were found. We further observed that *F. nucleatum* can bind to many different tumor types in cell line-based assays. In humans, *F. nucleatum* might have a special tropism for human colon adenocarcinoma and its abundance in the oral cavity might provide easy access to the gastrointestinal tract. Perhaps microbiome surveys of other malignant tumors will reveal an enrichment of *F. nucleatum* as well.

We observed only partial restoration of primary NK cell cytotoxicity when we used TIGIT-Ig to block *F. nucleatum*-TIGIT interactions. Killing might only have been partially restored with TIGIT-Ig because this reagent does not efficiently block *F. nucleatum*-TIGIT interactions. Indeed, in the absence of Fap2, inhibition of NK cell cytotoxicity was abrogated completely.

We were unable to use a blocking anti-hTIGIT mAb that we had previously generated, because this mAb was unable to block the *F. nucleatum*-TIGIT interaction. This result suggests that TIGIT interacts with *F. nucleatum* at a binding site distinct from that of hPVR. However, we did observe that the inhibition of NK cell cytotoxicity was mediated via the same signaling motifs required for the inhibition of TIGIT by PVR. Other PVR binding receptors such as DNAM1 did not interact with *F. nucleatum*.

Using transposon-based mutagenesis we found two *F. nucleatum* mutants that could not inhibit killing by YTS TIGIT cells. The transposon was inserted in the *fap*2 gene and using NK cytotoxicity assays, BW reporter assays, ELISA-based binding assays, and Western blotting, we found that TIGIT interacts with Fap2.

The Fap2 protein undoubtedly possesses functions beyond hTIGIT binding. Indeed, we found that Fap2 is involved in the binding of *F. nucleatum* to cell lines such as K562 and RKO. In addition, we observed that Fap2 is involved in *F. nucleatum*-mediated hemagglutination, in co-aggregation with other bacteria, and in placental colonization in mice (Coppenhagen-Glazer et al., 2015). The hemagglutination potency of Fap2 directly correlated with TIGIT inhibition. Furthermore, the 726 bacterium showed unstable hemagglutination properties and sometimes after few passages in culture lost its hemagglutination ability. In these situations, no TIGIT inhibition was observed. Going forward, it will be interesting to determine the exact Fap2 domain(s) involved in hemagglutination and TIGIT inhibition, to investigate why strains vary in hemagglutination,

and to precisely understand how *F. nucleatum* hemagglutination activity is related to *F. nucleatum* Fap2-TIGIT interactions.

F. nucleatum undoubtedly possesses other molecules that can mediate its binding to host cells. In support of this idea, there is the *Fusobacterium* adhesin, FadA (Xu et al., 2007), as well as our observations that binding of Fap2 mutants to 721.221 cells was similar to that of the wild-type *F. nucleatum* and both wildtype and mutant *F. nucleatum* strains bound TIGIT-negative human cell lines.

In summary, we have identified a tumor-based immune evasion mechanism that is bacteria-dependent, wherein *F. nucleatum* bound tumors are protected from NK-mediated killing and immune cell attack due to an interaction between the fusobacterial protein Fap2 with the immune cells inhibitory receptor TIGIT.

EXPERIMENTAL PROCEDURES

Primary Human NK Cells, TILs, DC, Cell Lines, Fusion Proteins, and Antibodies

Primary human NK cells were isolated from PBLs of healthy donors, using the human NK cell isolation kit and the autoMACS instrument according to the manufacturer's instructions (Miltenyi Biotec). NK cell purity was 99% as determined by positive CD56 and NKp46 expression and negative CD3 expression. DCs were generated as previously described (Verbovetski et al., 2002). Melanoma tumor lines and TILs were obtained from patients as previously described (Besser et al., 2013). IRB approval and patient consent to obtain human tumor tissue was obtained. Use of human samples was approved by the IRB of Harvard Medical School, Tel Hashomer Hospital, and Hadassah Medical School. The following cell lines were used: the human EBV transformed 721.221 cells, the human colorectal line RKO, the human erythroleukemia line K562, the mouse thymoma BW cells and the NK tumor cell line YTS ECO. The generation of the various YTS ECO transfectants YTS hTIGIT, YTS STOP 190, and YTS STOP 231 cells was described previously (Stanietsky et al., 2009). The generation of the BW transfectants BW hTIGIT, BW mTIGIT, and BW NKp30 was described previously (Stanietsky et al., 2013; Stanietsky et al., 2009). All cells, except from the human primary NK cells, were grown in RPMI medium supplemented with 10% FCS. Human NK cells were grown in the presence of 10% human sera, supplemented with human IL-2. The generation of TIGIT-Ig, the blocking anti-TIGIT mAb #4, and the control-Ig fusion proteins was previously described (Stanietsky et al., 2013; Stanietsky et al., 2009). The following commercial antibodies were used: anti-mouse TIGIT (FAB7267A, R&D systems), anti-NKp30 (clone P30-15, Biolegend), and anti-human PVR (MAB25301, R&D systems).

Bacterial Strains and Growth Conditions

F. nucleatum strains were grown in Wilkins Chalgren broth (Oxoid) or on Columbia agar plates (Oxoid, UK) supplemented with 5% defibrinated sheep blood (Novamed) in an anaerobic chamber (Bactron I-II Shellab) in an atmosphere of 90% N_2, 5% CO_2 and 5% H_2 at 37°C. *Escherichia coli* were grown in LB broth (Difco) or on LB agar plates (Difco), under aerobic conditions at 37°C. All antimicrobials used in this study were purchased from

Sigma-Aldrich Israel. Antibiotic concentrations were as follows: ampicillin 100 μg μl^{-1}, chloramphenicol 30μg ml^{-1}, and thiamphenicol 5μg ml^{-1}. For fusobacteria, broth was supplemented with half concentrations. Clinical tumor isolates (CTI) were isolated from human colon adenocarcinomas. Tumors were resected and a portion of the tumor was placed in tryptic soy broth with 0.05% cysteine-hydrochloride. Tumors were disaggregated and the tissue was plated on Fastidious Anaerobe agar plates supplemented with josamycin, vancomycin, and norfloxaxin (3,4, and 1 μg/ml, respectively). Colonies were streaked for re-isolation on Columbia agar and subjected to Gram-staining before 16S rRNA gene based sequencing for identification. *F. nucleatum* CTIs have been deposited at BEI resources repository (http://www.beiresources.org/). Transposon mutagenesis of *F. nucleatum* and the determination of the transposon insertion site in the fusobacterial genome was performed as recently described (Coppenhagen-Glazer et al., 2015).

FITC Labeling of Bacteria and Binding to Cells

F. nucleatum (10^9 CFU/ml) was labeled with fluorescein isothiocyanate (FITC) (0.1 mg/ml in PBS; Sigma-Aldrich) for 30 min at room temperature and washed three times in PBS. FITC labeled bacteria were incubated with various cells at various bacteria to cell ratios for 30 min at 4°C. Cells were washed and bacterium binding was detected using flow cytometry.

Killing Assays

Target cells were grown overnight in the presence of ^{35}S-Methionine added to a methionine-free media (Sigma). Prior to incubation with the effectors cells (either TILs or NK cells), cells were washed, counted, and 5,000 cells/well were plated. When target cells were coated with bacteria, the bacterial-to-target ratio was 600:1. When fusion proteins were included in the assays, each well received 5 μg of the appropriate protein. When antibodies were included, each well received 0.5 μg of mAb. For each target, the spontaneous ^{35}S release was calculated using cells, which were not incubated with effector cells, and maximum [^{35}S]-release was calculated by applying 100 μl 0.1 M NaOH to the target cells. The amount of [^{35}S]-release was measured after 5 hr of incubation with effectors (at 37°C) by a MicroBeta2 2450 (Perkin Elmer). The cytotoxicity of the melanoma TILs was determined after 12 hr of incubation with their appropriate targets. The maximum and spontaneous release of ^{35}S did not change in the presence or in the absence of the various bacteria.

BW Assays

The various bacteria were placed in 96 well plates and incubated for 1 hr at 37°C in medium containing RPMI supplemented with 10% FCS and penicillin-streptomycin. Subsequently, cells (50,000 of the appropriate BW or BW transfectants) were added and incubated together with the bacteria for 48 hr at 37°C, 5% CO2. The final cell to bacteria ratio was 1:300. Next, supernatants were collected and the presence of mouse IL-2 in the supernatants was determined using standard ELISA assay.

T Cell Proliferation Assays

T cells were isolated from peripheral blood of CMV-positive and CMV-negative people. 100,000 T cells were plated in each well of 96 round bottom plates incubated with 0.6 μg dissolved in 50% DMSO (in PBS) of pp65 overlapping peptides PepMix HCMVA (pp65), (JPT Peptide Technologies), in the presence or in the absence of various bacteria (bacteria-to-target ratio was 300:1). Plates were incubated for 48 hr and then the presence of IFN-γ in the cell culture supernatants was determined by ELISA.

IL-12 Secretion from DCs following Bacteria Stimulation

DCs were isolated from peripheral blood as described above. 100,000 T cells were plated in each well of 96 round bottom plates incubated in the presence or in the absence of various bacteria, at various bacteria to DC ratios. Plates were incubated for 48 hr and then the presence of IL-12 in the cell culture supernatants was determined by ELISA.

ELISA Assays for Direct TIGIT Binding

Various bacteria (0.5×10^6 per well) were incubated overnight in 100 μl of binding solution (0.1 M Na_2HPO_4, pH 9). Plates were then blocked with 2% milk in PBS, washed, and incubated for 2 hr with TIGIT-Ig proteins (3 μg protein per well). Binding of the Ig fusion protein was detected using biotinylated anti-human antibodies (the TIGIT-Ig fusion protein is composed of the extracellular portion of human TIGIT fused to human IgG1 (Stanietsky et al., 2009). ELISA assays were performed with streptavidin-HRP.

Immunofluorescence Staining

Slides were defrosted and fixated in 4% PFA. Samples were permeabilized with 0.1% Triton in PBS, washed, and blocked in Cas BlockTM (Invitrogen) at room temperature. Slides were then incubated with primary anti-TIGIT antibody (mAb #1, in-house prepared, 1:10 dilution) overnight and then were incubated with Alexa-Fluor 647 conjugated goat anti-mouse antibodies directed at the IgG (H+L) part of the primary antibody. Nuclear staining was performed using DAPI staining according to manufacturer protocol (Sigma-Aldrich).

Outer Membrane Vesicle Preparation

Four-day-old *F. nucleatum* cultures were harvested by centrifugation at $10,000 \times g$ for 20 min at 4°C. Culture supernatants were collected and filtered through a 0.2 μm filter (Whatman Schleicher & Schuell). Cell-free supernatants were centrifuged at $100,000 \times g$ for 2 hr. The supernatant was discarded and the pellet containing the vesicles was washed twice with Tris-buffered saline (TBS, 0.05 M Tris-HCl [pH 7.8], 0.1 M NaCl) by centrifugation at $100,000 \times g$. The pellet was stored at −20°C until further use.

Supplementary Material

Refer to Web version on PubMed Central for supplementary material.

ACKNOWLEDGMENTS

REFERENCES

Besser MJ, Shapira-Frommer R, Itzhaki O, Treves AJ, Zippel DB, Levy D, Kubi A, Shoshani N, Zikich D, Ohayon Y, et al. Adoptive transfer of tumor-infiltrating lymphocytes in patients with metastatic melanoma: intent-to-treat analysis and efficacy after failure to prior immunotherapies. Clinical cancer research: an official journal of the American Association for Cancer Research. 2013; 19:4792–4800. [PubMed: 23690483]

Castellarin M, Warren RL, Freeman JD, Dreolini L, Krzywinski M, Strauss J, Barnes R, Watson P, Allen-Vercoe E, Moore RA, Holt RA. *Fusobacterium nucleatum* infection is prevalent in human colorectal carcinoma. Genome Res. 2012; 22:299–306. [PubMed: 22009989]

Chaushu S, Wilensky A, Gur C, Shapira L, Elboim M, Halftek G, Polak D, Achdout H, Bachrach G, Mandelboim O. Direct recognition of *Fusobacterium nucleatum* by the NK cell natural cytotoxicity receptor NKp46 aggravates periodontal disease. PLoS Pathog. 2012; 8:e1002601. [PubMed: 22457623]

Coley WB. The Treatment of Inoperable Sarcoma by Bacterial Toxins (the Mixed Toxins of the *Streptococcus erysipelas* and the *Bacillus prodigiosus*). Proc. R. Soc. Med. 1910; 3:1–48. Surg Sect. [PubMed: 19974799]

Coppenhagen-Glazer S, Sol A, Abed J, Naor R, Zhang X, Han YW, Bachrach G. Fap2 of *Fusobacterium nucleatum* is a galactose inhibitable adhesin, involved in coaggregation, cell adhesion and preterm birth. Infect. Immun. 2015 Published online January 5, 2015. http://dx.doi.org/10.1128/IAI.02838-14.

Elias S, Yamin R, Golomb L, Tsukerman P, Stanietsky-Kaynan N, Ben-Yehuda D, Mandelboim O. Immune evasion by oncogenic proteins of acute myeloid leukemia. Blood. 2014; 123:1535–1543. [PubMed: 24449212]

Gardiner CM. Killer cell immunoglobulin-like receptors on NK cells: the how, where and why. Int. J. Immunogenet. 2008; 35:1–8. [PubMed: 18093180]

Gonen-Gross T, Goldman-Wohl D, Huppertz B, Lankry D, Greenfield C, Natanson-Yaron S, Hamani Y, Gilad R, Yagel S, Mandelboim O. Inhibitory NK receptor recognition of HLA-G: regulation by contact residues and by cell specific expression at the fetal-maternal interface. PLoS ONE. 2010; 5:e8941. [PubMed: 20126612]

Grange JM, Bottasso O, Stanford CA, Stanford JL. The use of mycobacterial adjuvant-based agents for immunotherapy of cancer. Vaccine. 2008; 26:4984–4990. [PubMed: 18625281]

Han YW, Wang X. Mobile microbiome: oral bacteria in extra-oral infections and inflammation. J. Dent. Res. 2013; 92:485–491. [PubMed: 23625375]

Han YW, Redline RW, Li M, Yin L, Hill GB, McCormick TS. *Fusobacterium nucleatum* induces premature and term stillbirths in pregnant mice: implication of oral bacteria in preterm birth. Infect. Immun. 2004; 72:2272–2279. [PubMed: 15039352]

Hanahan D, Weinberg RA. Hallmarks of cancer: the next generation. Cell. 2011; 144:646–674. [PubMed: 21376230]

Jobin C. Colorectal cancer: looking for answers in the microbiota. Cancer discovery. 2013; 3:384–387. [PubMed: 23580283]

Koch J, Steinle A, Watzl C, Mandelboim O. Activating natural cytotoxicity receptors of natural killer cells in cancer and infection. Trends Immunol. 2013; 34:182–191. [PubMed: 23414611]

Kostic AD, Gevers D, Pedamallu CS, Michaud M, Duke F, Earl AM, Ojesina AI, Jung J, Bass AJ, Tabernero J, et al. Genomic analysis identifies association of *Fusobacterium* with colorectal carcinoma. Genome Res. 2012; 22:292–298. [PubMed: 22009990]

Kostic AD, Chun E, Robertson L, Glickman JN, Gallini CA, Michaud M, Clancy TE, Chung DC, Lochhead P, Hold GL, et al. *Fusobacterium nucleatum* potentiates intestinal tumorigenesis and modulates the tumor-immune microenvironment. Cell Host Microbe. 2013; 14:207–215. [PubMed: 23954159]

Lankry D, Gazit R, Mandelboim O. Methods to identify and characterize different NK cell receptors and their ligands. Methods Mol. Biol. 2010; 612:249–273. [PubMed: 20033646]

Lee P, Tan KS. *Fusobacterium nucleatum* activates the immune response through retinoic acid-inducible gene I. J. Dent. Res. 2014; 93:162–168. [PubMed: 24334410]

Liu H, Redline RW, Han YW. *Fusobacterium nucleatum* induces fetal death in mice via stimulation of TLR4-mediated placental inflammatory response. J. Immunol. 2007; 179:2501–2508. [PubMed: 17675512]

Liu S, Zhang H, Li M, Hu D, Li C, Ge B, Jin B, Fan Z. Recruitment of Grb2 and SHIP1 by the ITT-like motif of TIGIT suppresses granule polarization and cytotoxicity of NK cells. Cell Death Differ. 2013; 20:456–464. [PubMed: 23154388]

Rubinstein MR, Wang X, Liu W, Hao Y, Cai G, Han YW. *Fusobacterium nucleatum* promotes colorectal carcinogenesis by modulating E-cadherin/β-catenin signaling via its FadA adhesin. Cell Host Microbe. 2013; 14:195–206. [PubMed: 23954158]

Sears CL, Garrett WS. Microbes, microbiota, and colon cancer. Cell Host Microbe. 2014; 15:317–328. [PubMed: 24629338]

Seidel E, Glasner A, Mandelboim O. Virus-mediated inhibition of natural cytotoxicity receptor recognition. Cellular and molecular life sciences. Cell. Mol. Life Sci. 2012; 69:3911–3920.

Sobhani I, Tap J, Roudot-Thoraval F, Roperch JP, Letulle S, Langella P, Corthier G, Tran Van Nhieu J, Furet JP. Microbial dysbiosis in colorectal cancer (CRC) patients. PLoS ONE. 2011; 6:e16393. [PubMed: 21297998]

Stanietsky N, Simic H, Arapovic J, Toporik A, Levy O, Novik A, Levine Z, Beiman M, Dassa L, Achdout H, et al. The interaction of TIGIT with PVR and PVRL2 inhibits human NK cell cytotoxicity. Proc. Natl. Acad. Sci. USA. 2009; 106:17858–17863. [PubMed: 19815499]

Stanietsky N, Rovis TL, Glasner A, Seidel E, Tsukerman P, Yamin R, Enk J, Jonjic S, Mandelboim O. Mouse TIGIT inhibits NK-cell cytotoxicity upon interaction with PVR. Eur. J. Immunol. 2013; 43:2138–2150. [PubMed: 23677581]

Strauss J, Kaplan GG, Beck PL, Rioux K, Panaccione R, Devinney R, Lynch T, Allen-Vercoe E. Invasive potential of gut mucosa-derived *Fusobacterium nucleatum* positively correlates with IBD status of the host. Inflamm. Bowel Dis. 2011; 17:1971–1978. [PubMed: 21830275]

Tannock GW. The search for disease-associated compositional shifts in bowel bacterial communities of humans. Trends Microbiol. 2008; 16:488–495. [PubMed: 18783952]

Témoin S, Chakaki A, Askari A, El-Halaby A, Fitzgerald S, Marcus RE, Han YW, Bissada NF. Identification of oral bacterial DNA in synovial fluid of patients with arthritis with native and failed prosthetic joints. J. Clin. Rheumatol. 2012; 18:117–121. [PubMed: 22426587]

Verbovetski I, Bychkov H, Trahtemberg U, Shapira I, Hareuveni M, Ben-Tal O, Kutikov I, Gill O, Mevorach D. Opsonization of apoptotic cells by autologous iC3b facilitates clearance by immature dendritic cells, down-regulates DR and CD86, and up-regulates CC chemokine receptor 7. J. Exp. Med. 2002; 196:1553–1561. [PubMed: 12486098]

Vivier E, Raulet DH, Moretta A, Caligiuri MA, Zitvogel L, Lanier LL, Yokoyama WM, Ugolini S. Innate or adaptive immunity? The example of natural killer cells. Science. 2011; 331:44–49. [PubMed: 21212348]

Xu M, Yamada M, Li M, Liu H, Chen SG, Han YW. FadA from *Fusobacterium nucleatum* utilizes both secreted and nonsecreted forms for functional oligomerization for attachment and invasion of host cells. J. Biol. Chem. 2007; 282:25000–25009. [PubMed: 17588948]

Highlights

- NK cell killing of tumors is inhibited by hemagglutinating *F. nucleatum* strains

- Immune cell activities are inhibited by *F. nucleatum* via its Fap2 protein

- The Fap2 protein interacts with TIGIT and inhibits immune cell activities
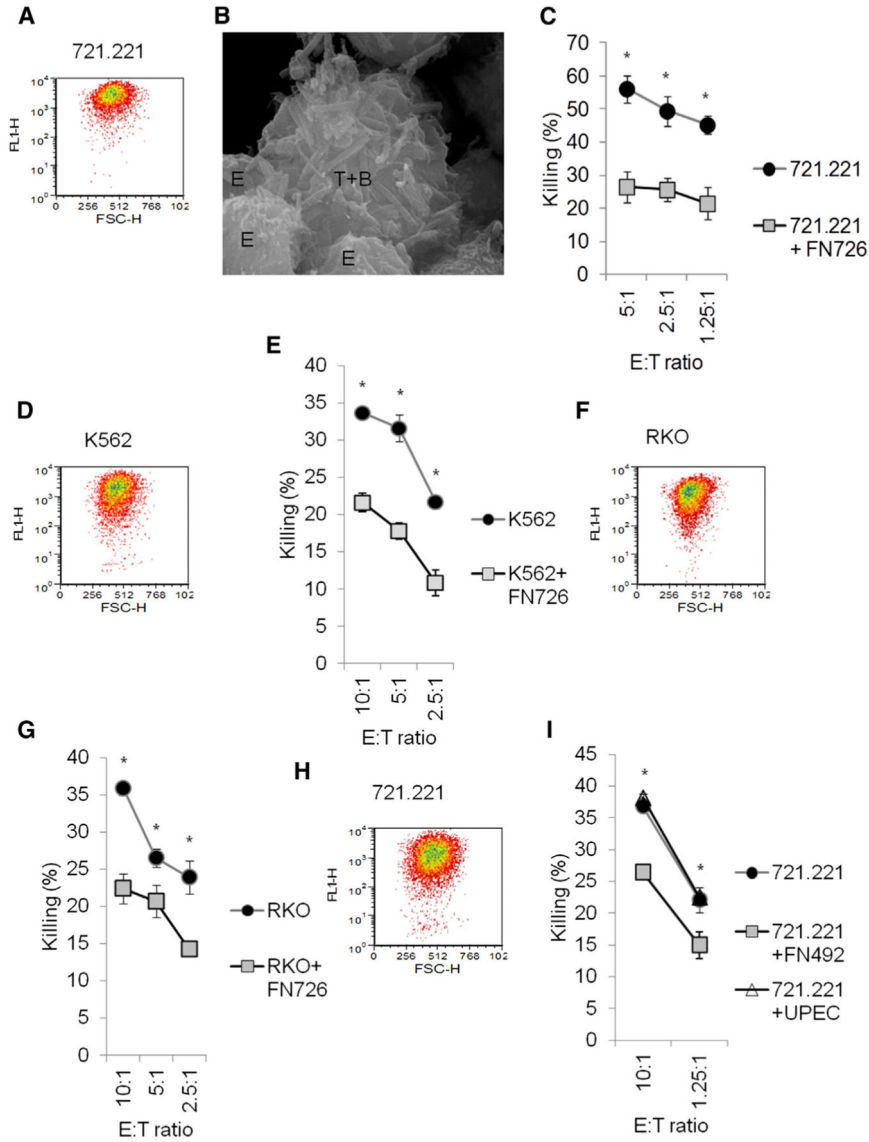
**Figure 1. *F. nucleatum* Protects Tumor Cells from NK Cell Killing**

(A, D, F, and H) Flow cytometry of FITC-labeled *F. nucleatum* strains: 23726 (726) (A, D, and F) and 49256 (492) (H) binding to 721.221 (A and H), K562 (D), RKO (F). Figure shows one representative staining out of four performed.

(B) SEM of human NK cells (Effector-E) incubated with 721.221 (Target-T) cells coated with the 726 bacterial strain (Bacteria-B). The bacteria to 721.221 ratio was 600:1.

(C, E, G, and I) NK cytotoxicity assays were performed on ^{35}S-labeled 721.221 (C and I), K562 (E) and RKO (G) cells incubated without or with the 726 strain (C, E, and G, designated +FN726), the 492 *F. nucleatum* strain (I, designated +FN492) and with UPEC strain CFT073 (I, designated +UPEC). The bacteria to cells ratio was 600:1. The various cells incubated with and without the bacteria were incubated with primary activated human NK cells for 5 hr and at various Effector to Target (E:T) ratios indicated on the x axis.

Figure shows one representative experiment out of three performed. *p < 0.05 for (C), (E), (G), and (I). The error bars are derived from triplicates.
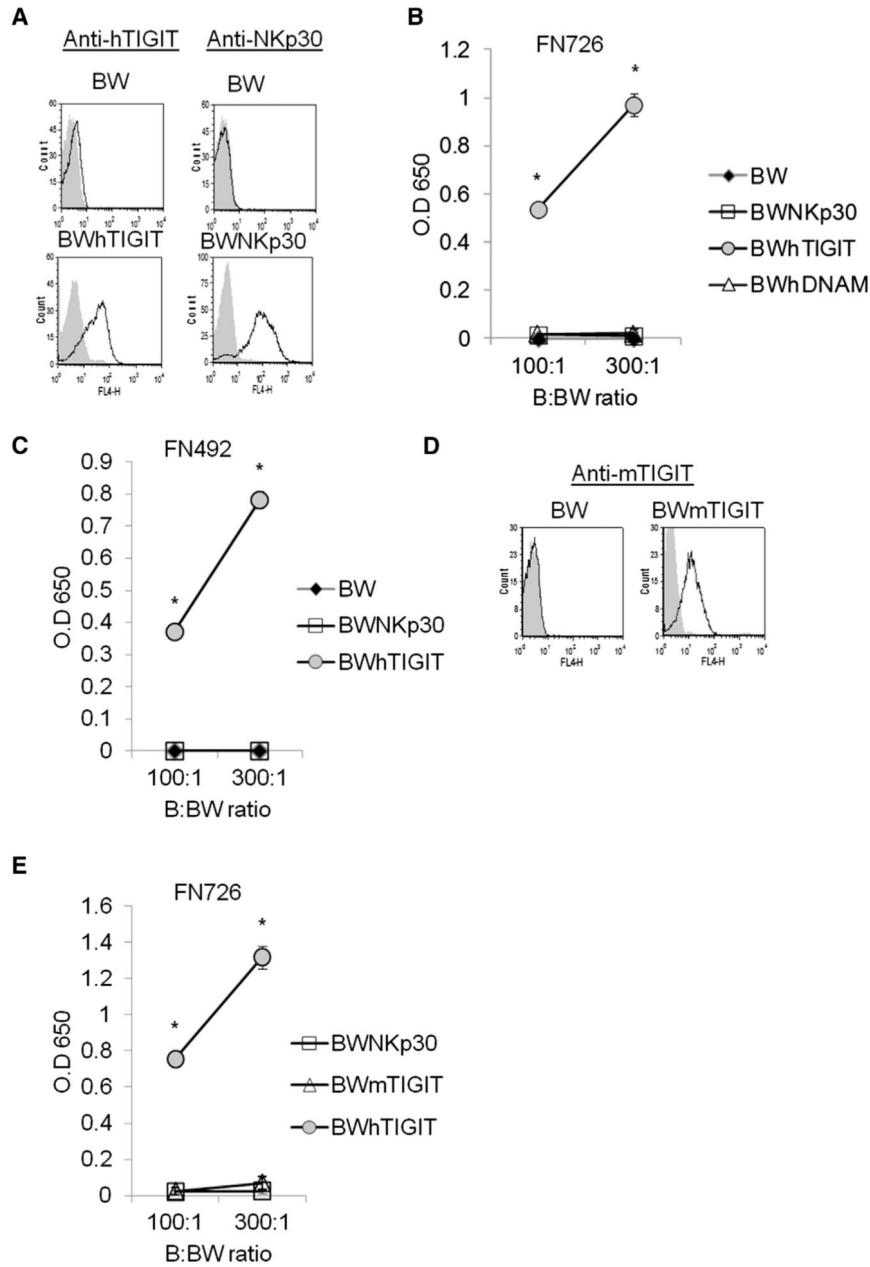
Figure 2. *F. nucleatum* Interacts with TIGIT

(A and D) Flow cytometry of parental BW cells of BW cells transfected with human TIGIT fused to mouse CD3 zeta chain (BW hTIGIT, A), of BW cells transfected with human NKp30 fused to mouse CD3 zeta chain (BW NKp30, A) and of BW cells transfected with murine TIGIT fused to mouse CD3 zeta chain (BW mTIGIT, D). The various BW cells were stained with the antibodies indicated above the histograms. The gray filled histograms represent the control staining with the secondary antibody only. The various BW cells that are indicated in the figure were incubated with *F. nucleatum* 726 (B and E) or with *F. nucleatum* 492 (C) at bacteria to BW (B:BW) ratios that are indicated in the x axis. Mouse IL-2 in the supernatants was determined by ELISA. Figure shows one representative

experiment out of six performed. *p < 0.001 for (B), (C), and (E). The error bars are derived from triplicates.
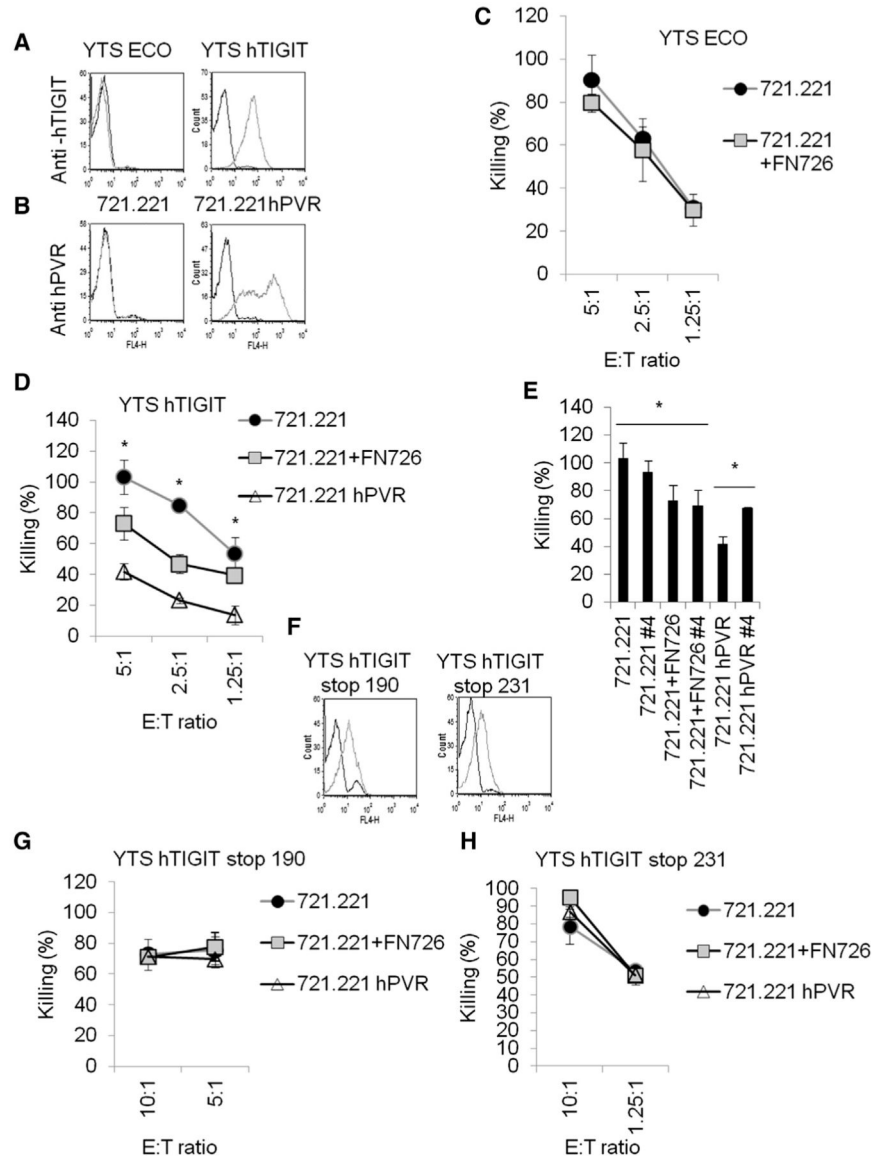
Figure 3. *F. nucleatum* Inhibits YTS Cytotoxicity via TIGIT

(A) Flow cytometry of parental YTS ECO and of YTS ECO cells expressing human TIGIT (YTS hTIGIT) stained with anti-human TIGIT (gray empty histograms) or with secondary control antibodies only (black empty histograms).

(B) Flow cytometry of parental 721.221 and of 721.221 cells expressing human PVR (721.221hPVR) stained with anti-human PVR (gray empty histograms) or with secondary control antibodies only (black empty histograms). For (A) and (B), one representative staining out of three performed is shown.

(C and D) YTS ECO (C) and YTS hTIGIT (D) cells were incubated with ^{35}S-labeled 721.221 cells (C and D) or with 721.221 hPVR cells (D). The cells were pre-incubated or not with the *F. nucleatum* 726 (designated 721.221+FN726). The bacteria to cells ratio was 600:1. Incubation was performed for 5 hr at the various YTS:Target (E:T) ratios shown on

the x axis. Figure shows one representative experiment out of four performed. *p < 0.05. The error bars are derived from triplicates.

(E) YTS hTIGIT cells were incubated with or without anti-human TIGIT mAb #4 (#4) and then incubated with ^{35}S-labeled 721.221 cells (721.221), with 721.221 cells that were pre-incubated with *F. nucleatum* 726 (721.221 FN726, bacterium to cells ratio of 600:1) or with 721.221 cells expressing human PVR (721.221 hPVR). The E:T ratio was 5:1 and incubations were performed for 5 hr. *p < 0.05. The error bars are derived from triplicates.

(F) Flow cytometry of parental YTS ECO cells expressing TIGIT in which a STOP mutation was inserted in amino acid number 190 (YTS hTIGIT stop 190) or in amino acid 231 TIGIT (YTS hTIGIT stop 231), stained with anti-human TIGIT (gray empty histograms) or with secondary control antibodies only (black empty histograms). Figure shows one representative experiment of three performed.

(G and H) YTS hTIGIT stop 190 (G) and YTS hTIGIT stop 231 (H) cells were incubated with ^{35}S-labeled 721.221 cells that were pre-incubated with or without *F. nucleatum* 726 (designated 721.221 FN726) or with 721.221 hPVR. The bacteria to cells ratio was 600:1. Incubation was performed for 5 hr at the various E:T ratios that are indicated in the x axis. Figure shows one representative experiment out of two performed. The error bars are derived from triplicates.
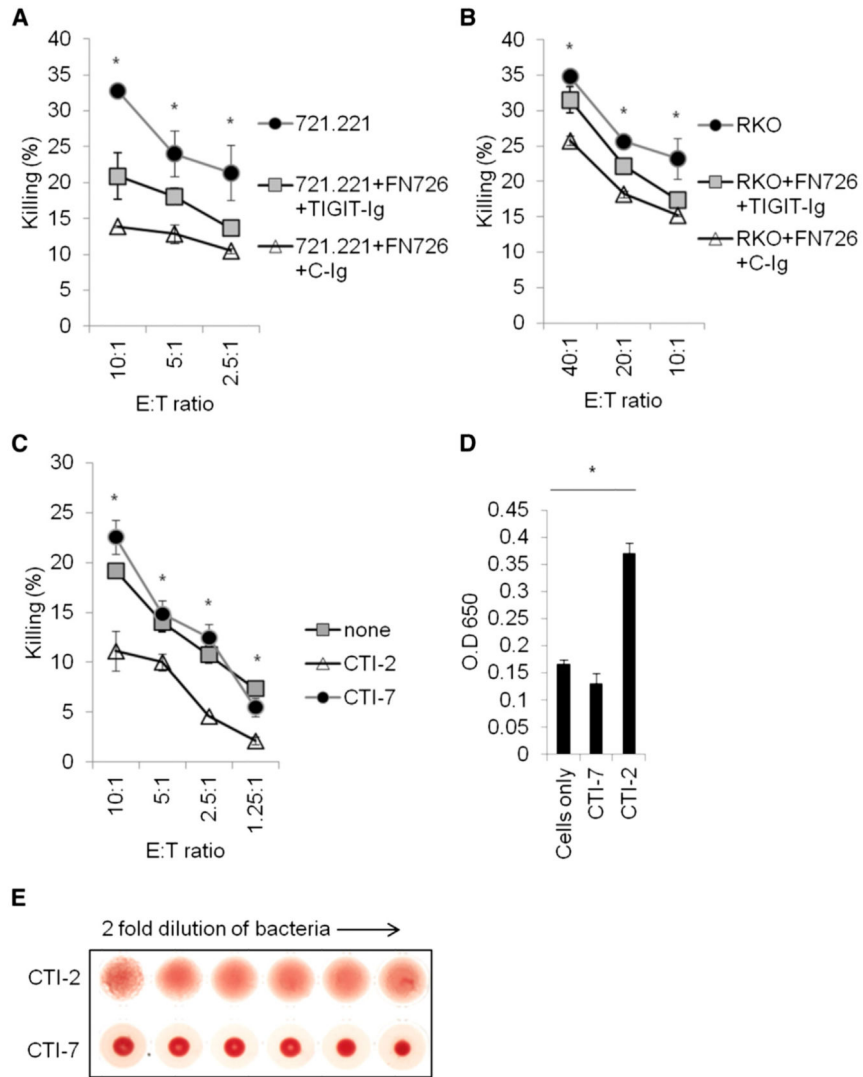
Figure 4. *F. nucleatum* Inhibits Primary NK Cytotoxicity via TIGIT in an Hemagglutination-Dependent Manner

(A and B) NK cytotoxicity assays were performed on ^{35}S-labeled 721.221 (A) and RKO (B) cells incubated with or without *F. nucleatum* 726 (designated 721221+FN726 and RKO +FN726) and then incubated with or without TIGIT-Ig or control Ig (C-Ig) fusion proteins. The bacteria:cell ratio was 600:1. The various cells were then incubated with primary human NK cells for 5 hr and at various E:T ratios indicated on the x axis. Figure shows one representative experiment out of 2 performed. *p < 0.05 for 721.221 and RKO cells relative to cells with *F. nucleatum* and TIGIT-Ig or control-Ig. The error bars are derived from triplicates.

(C) YTS TIGIT cells were incubated with 721.221 cells that were pre-incubated or not with the clinical *F. nucleatum* strains CTI-7 and CTI-2 isolated from human colon adenocarcinomas. *p < 0.001. The error bars are derived from triplicates.

(D) BW hTIGIT cells were incubated with the two clinical strains CTI-7 and CTI-2 at bacteria: BW ratio of 300:1. Mouse IL-2 in the supernatants was determined by ELISA. *p < 0.05. The error bars are derived from triplicates.

(E) Fifty microliters of human red blood cells (2% in PBS) were incubated with 50 μl of two fold serial dilutions (in PBS) of the indicated bacteria (original O.D was 1). Hemagglutination was evaluated following 120 min incubation at room temperature. Figure shows one representative experiment out of three performed.
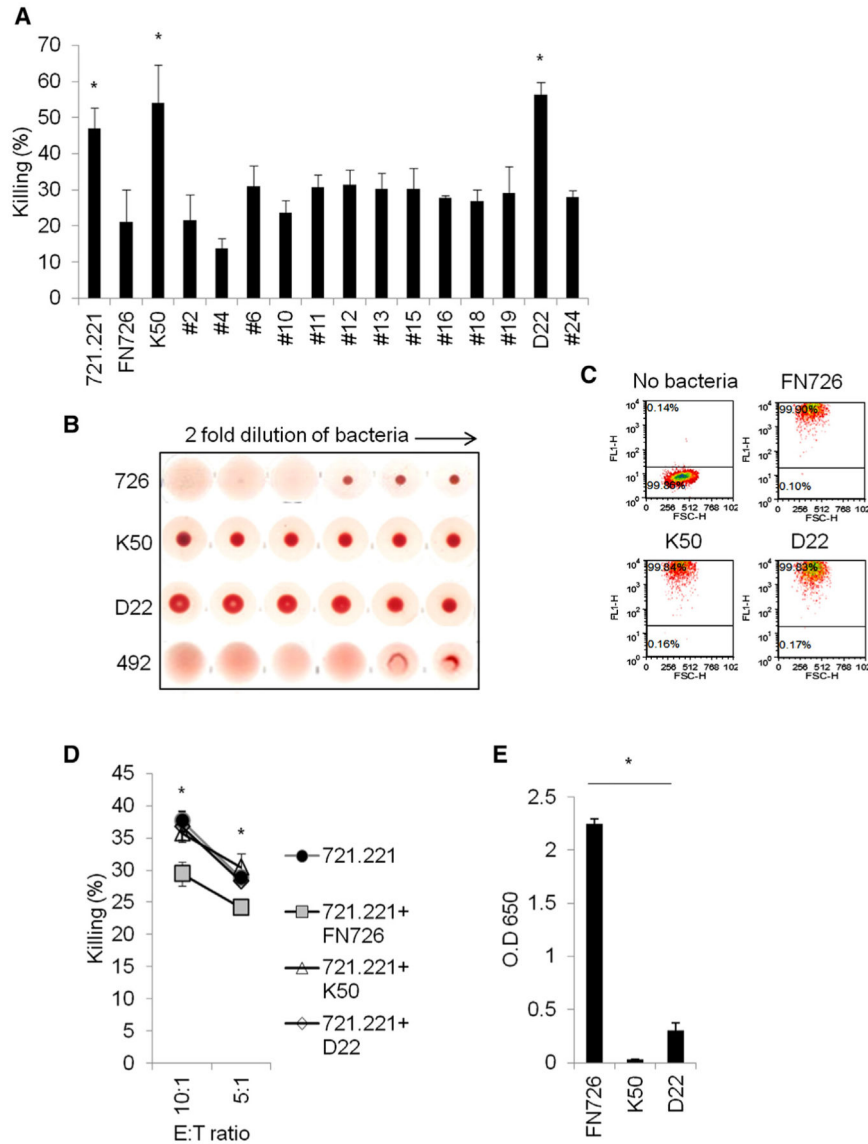
Figure 5. Identification of Two Mutants Defective in Their Ability to Inhibit Killing and to Hemagglutinate Red Blood Cells

(A) YTS hTIGIT cells were incubated with ^{35}S-labeled 721.221 cells and with 721.221 cells that were pre-incubated with or without the wild-type *F. nucleatum* 726 (designated FN726) or with mutants generated in the *F. nucleatum* 726 (designated with numbers, the two non-inhibitory mutants K50 and D22 are designated with letters and number). The bacteria to cells ratio was 600:1. Incubation was performed for 5 hr at an E:T ratio of 5:1. Figure shows several randomly selected mutants. *p < 0.0005. The error bars are derived from triplicates.

(B) Fifty microliters of human red blood cells (2% in PBS) were incubated with 50 μl of two fold serial dilutions (in PBS) of the indicated bacteria (original O.D was 1). Hemagglutination was evaluated following 120 min incubation at room temperature.

(C) Flow cytometry of FITC-labeled wild-type 726 bacterium and mutants K50 and D22 binding to 721.221 cells. The bacteria to 721.221 ratio was 600:1. The left top dot plot

shows 721.221 cells without bacteria. The percentages of binding are indicated in the figure. See also Figure S1. Figure shows one representative experiment out of three performed.

(D) NK cytotoxicity assays were performed on ^{35}S-labeled 721.221 cells incubated without or with *F. nucleatum* 726 (designated 721221+FN726) and with the two mutants K50 and D22 (designated 721221+K50 and 721221+D22, respectively). The bacteria to cell ratio was 600:1. The various cells were then incubated with primary activated human NK cells for 5 hr and at various E:T ratios indicated on the x axis. Figure shows one representative experiment out of three performed. *p < 0.005. The error bars are derived from triplicates.

(E) BWhTIGIT cells were incubated with *F. nucleatum* 726 and with the two *F. nucleatum* mutants K50 and D22 at bacterium to BW ratio of 300:1. Mouse IL-2 in the supernatants was determined using ELISA. Figure shows one representative experiment out of three performed. *p < 0.0005. The error bars are derived from triplicates.
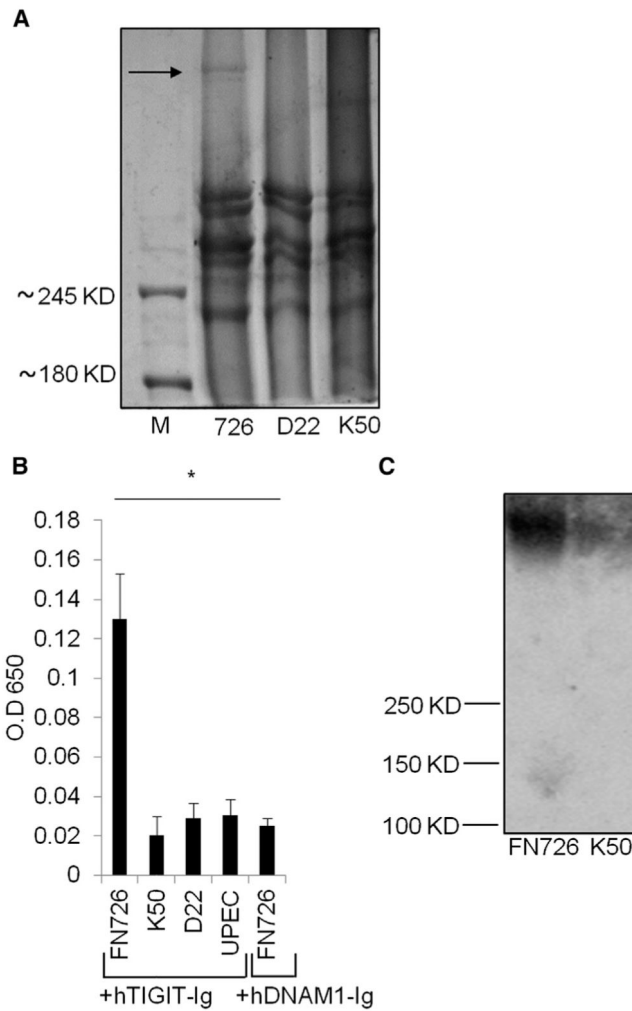
Figure 6. TIGIT Interacts with the Fap2 Protein of *F. nucleatum*

(A) SDS PAGE gel of membrane proteins purified from the wild-type *F. nucleatum* 726 strain and the two mutants: D22 and K50. The Fap2 protein bands present in the wild-type *F. nucleatum* 726 is indicated by an arrow. M represents the protein marker. The marker molecular weights are indicated on the left.

(B) 0.5×10^6 *F. nucleatum* 726, the *F. nucleatum* mutants K50 and D22 and the CFT073 UPEC were bound in wells of ELISA plates. Plates were incubated with human TIGIT-Ig or with human DNAM1-Ig (hDNAM1-Ig, incubated only with FN726) and ELISA assays were performed. Figure shows one representative experiment out of three performed. *p < 0.002. The error bars are derived from triplicates.

(C) Outer membrane vesicle proteins extracted from the wild-type *F. nucleatum* 726 and from K50 were run on a 7% SDS PAGE gel, transferred to a nitrocellulose membrane and incubated with TIGIT-Ig. The molecular weights protein markers are indicated on the left.
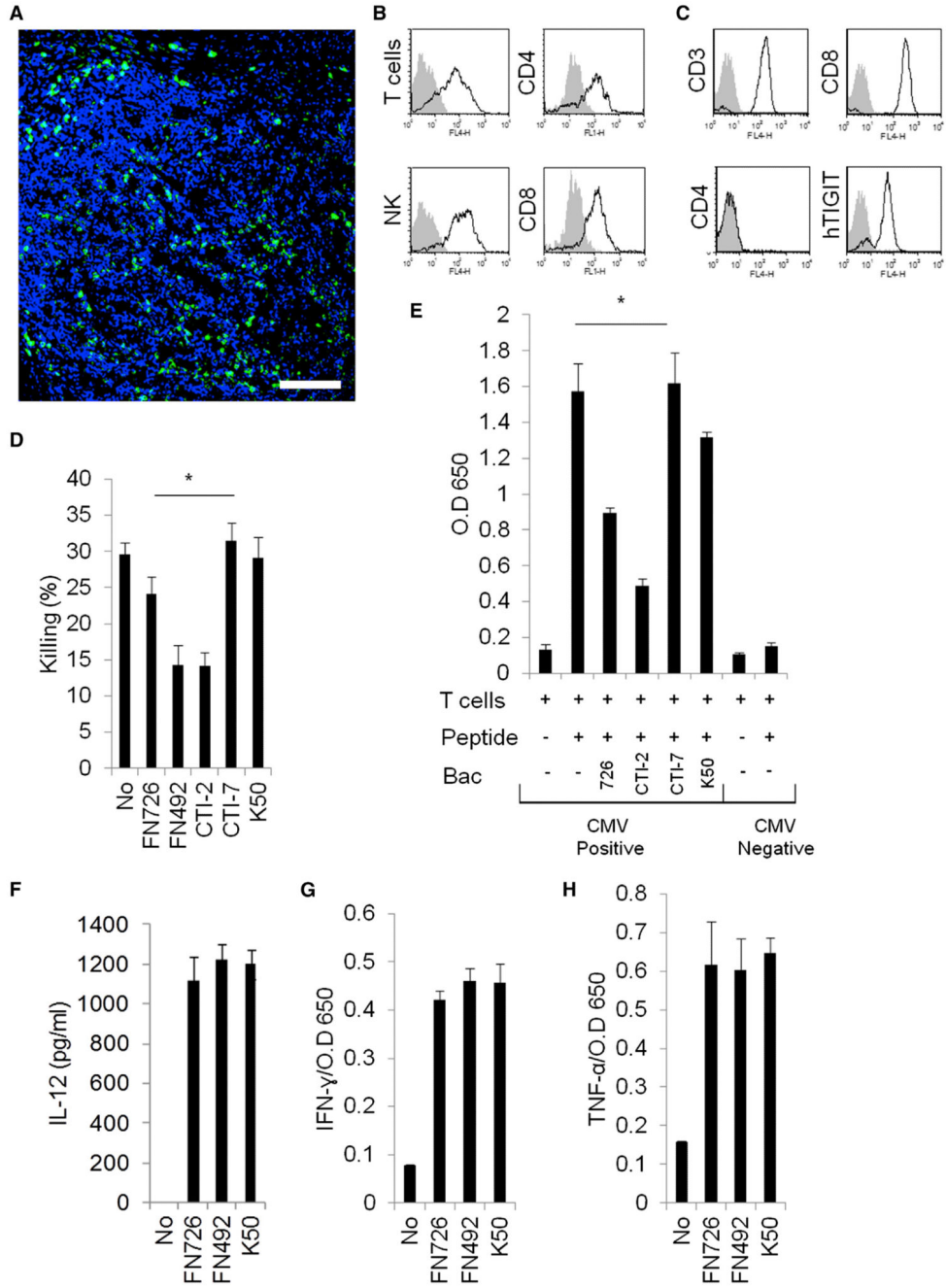
Figure 7. *F. nucleatum* Inhibits T Cell Activity

(A) Immunofluorescence microscopy of frozen sections derived from colon adenocarcinomas stained with anti-TIGIT mAb #1 (green) and DAPI (blue). Scale 100 μm.
(B) Tumor infiltrating lymphocytes were isolated from colon adenocarcinomas. The figure shows TIGIT expression (empty histograms) on the indicated tumor infiltrating lymphocytes: T cells, CD4+ T cells, CD8+ T cells, and NK cells. The filled histogram represents staining with control antibodies (APCconjugated for the T and NK cells and

FITC-conjugated for the CD4^{+} and CD8^{+} cells). The backgrounds were set on the entire lymphocyte population including both T and NK cells.

(C) Characterization of melanoma tumor-derived TIL #14. TIL-14 was stained with mAbs as indicated in the figure. The filled histogram represents the staining with control antibodies.

(D) TIL #14 cytotoxicity assays were performed on ^{35}S-labeled autologous melanoma #14 cells incubated without or with the various bacteria indicated on the x axis. The bacteria:cell ratio was 600:1. The E:T ratio was 5:1. *p < 0.05. The error bars are derived from triplicates.

(E) Lymphocytes isolated from CMV positive and CMV negative donors (indicated on the x axis), were incubated with or without a mixture of pp65 overlapping peptides and with or without the bacteria as indicated on the x axis. Incubation was performed for 48 hr and IFN-γ in the supernatants was determined by ELISA. *p < 0.005. The error bars are derived from triplicates.

(F) DC were incubated with or without the *F. nucleatum* strains indicated on the x axis at a bacteria to DC ratio of 100:1. IL-12 in the supernatants was determined by ELISA 48 hr later. The error bars are derived from triplicates.

(G and H) The supernatants obtained from (F), indicated on the x axis, were incubated with primary NK cells and the presence of IFN-γ (G) or TNF-α (H) in the supernatants was determined 48 hr later. The error bars are derived from triplicates.